SAND REPORT
SAND2002-2424
Unlimited Release
Printed August 2002

Evaluation of Design Concepts for Adaptive Wind Turbine Blades

Dayton Griffin, Principal Investigator
Global Energy Concepts, LLC
Kirkland, Washington 98109

Prepared by
Sandia National Laboratories
Albuquerque, New Mexico 87185 and Livermore, California 94550

Sandia is a multiprogram laboratory operated by Sandia Corporation, a Lockheed Martin Company, for the United States Department of Energy under Contract DE-AC04-94AL85000.

Sandia National Laboratories

Issued by Sandia National Laboratories, operated for the United States Department of Energy by Sandia Corporation.

Available to DOE and DOE contractors from
U.S. Department of Energy
Office of Scientific and Technical Information
P.O. Box 62
Oak Ridge, TN 37831

Telephone: (865)576-8401
Facsimile: (865)576-5728
E-Mail: reports@adonis.osti.gov
Online ordering: http://www.doe.gov/bridge

Available to the public from
U.S. Department of Commerce
National Technical Information Service
5285 Port Royal Rd
Springfield, VA 22161

Telephone: (800)553-6847
Facsimile: (703)605-6900
E-Mail: orders@ntis.fedworld.gov
Online order: http://www.ntis.gov/ordering.htm

SAND2002-2424
Unlimited Release
Printed August 2002

Evaluation of Design Concepts for Adaptive Wind Turbine Blades

Global Energy Concepts, LLC
5729 Lakeview Drive NE, #100
Kirkland, Washington 98109

Principal Investigator:
Dayton A. Griffin

Abstract

The objectives of this work were to develop conceptual structural designs for an adaptive (bend-twist coupled) blade, to evaluate candidate design concepts, to identify constraints and/or concerns for manufacturing, load paths, and stress concentrations, to develop estimates of structural performance and costs, and to select a single configuration as showing the greatest potential for success in manufacturing, strength and durability.

This report summarizes the work performed on this project, including the approach taken, configurations and materials considered, and the computational methodology used. The work presented includes:

- Candidate fiber orientations and fabric architectures for adaptive blade manufacture are identified and assessed on the basis of estimated static strength, stiffness, and fabrication costs.
- A parametric study is performed for potential blade structural arrangements. Each configuration is evaluated on the basis of estimated manufacturing cost and magnitude of bend-twist coupling achieved.
- Based on the parametric study results, a single configuration is selected for further evaluation. A complete blade model is developed and assessed on the basis of estimated manufacturing cost and bend-twist behavior under steady loading.

Acknowledgements

Sandia Technical Monitors: Thomas D. Ashwill
Paul S. Veers

This is a Contractor Report for Sandia National Laboratories that partially fulfills the deliverables under Contract #21010.

Table of Contents

1. Technical Approach

1.1 Overview

The objectives of this work were to develop conceptual structural designs for an adaptive (bend-twist coupled) blade, to evaluate candidate design concepts, to identify constraints and/or concerns for manufacturing, load paths, and stress concentrations, to develop estimates of structural performance and costs, and to select a single configuration as showing the greatest potential for success in manufacturing, strength and durability.

This report summarizes the work performed on this project, including the approach taken, configurations and materials considered, and the computational methodology used. The work presented includes:

- Candidate fiber orientations and fabric architectures for adaptive blade manufacture are identified and assessed on the basis of estimated static strength, stiffness, and fabrication costs.
- A parametric study is performed for potential blade structural arrangements. Each configuration is evaluated on the basis of estimated manufacturing cost and magnitude of bend-twist coupling achieved.
- Based on the parametric study results, a single configuration is selected for further evaluation. A complete blade model is developed and assessed on the basis of estimated manufacturing cost and bend-twist behavior under steady loading. That design is presently being evaluated via aeroelastic simulations under the WindPACT Rotor System Design Study.[1]

Based on the results and conclusions from this work, recommendations are made for follow-on work concerning adaptive blades.

1.2 Approach

The blade design used for this project was selected to be consistent with the WindPACT Blade System Design Study [2] and Rotor System Design Study. The baseline blade assumes a 1.5 MW rotor constructed of all-fiberglass prepreg laminate with no twist coupling. As many of the adaptive blades designs incorporate a carbon / fiberglass hybrid fiber arrangement, a secondary baseline design was developed with all-fiberglass prepreg skins and a carbon / fiberglass hybrid spar, again with no bend-twist coupling.

Several candidate design concepts were evaluated. Considerations include potential loads reduction, power performance, static and dynamic stability, structural efficiency, manufacturability and estimated fabrication costs. For each design considered, preliminary structural calculations were performed to size the required blade structure. The general process used was to:

- Develop a standardized loading that represents peak flapwise bending conditions.
- Estimate the design strains (static compression and tension) for the composite materials proposed using micromechanics and classical lamination theory.
- Construct an ANSYS model of a representative blade section using the NuMAD interface.[3]
- Use the ANSYS model to determine the schedule of plies required to sustain peak structural loads.
- Evaluate the resulting mass, stiffness, and extent of flap-twist coupling.
- Consult with manufacturers to identify candidate fabrication methods, estimate production costs, and identify potential difficulties in fabrication and/or obtaining structural robustness.

To evaluate candidate materials and structural layouts, a parametric study was performed using a constant cross-section shape that is representative of blade at the maximum chord location (25% span). Based on the parametric study results, a complete blade design was developed for a selected structural configuration.

1.3 Concepts Investigated

Two basic material types were evaluated for providing the bend-twist coupling. The first is a stitched hybrid fabric with carbon fibers oriented at a +20° angle (relative to the roll warp direction) and fiberglass fibers at a second orientation angle. For fabric stability and handling, a small amount of stabilizing fiber is assumed to be included in a third direction. The second material considered is a carbon preform constructed from non-continuous carbon fibers with a high degree of orientation. With these materials, the following structural arrangements were investigated.

1.3.1 Biased Skin with Conventional Unbiased Spar Caps

In this approach the skin provides the bend-twist coupling. The unbiased (fiberglass or hybrid carbon / fiberglass) spar caps provide the majority of the flapwise bending strength, but are intended to be relatively compliant in twisting. The 20° carbon fibers in the biased skin begin and end at the leading and trailing edges of the blade, leading to critical strains at those locations. In a detailed design, it is expected that the carbon fibers would be curtailed before reaching the trailing and leading edges to ameliorate this condition. However, for the present evaluation the biased skin is assumed to continue for the full chordwise extent.

1.3.2 Conventional Triaxial Skins with Biased Box Spar Caps

In this approach the flapwise bending strength and the bend-twist coupling are both supplied by the relatively thick spar caps, whereas the skins are made from conventional triaxial fiberglass material. In traditional blade design, the fibers at the upper and lower caps of this spar are primarily uniaxial while the remaining skins are made up of a minimal number of triaxial plies. In this type of design, the spar contributes most of the flapwise stiffness, but it contributes only about 50% of the torsional stiffness. Therefore, making a spar torsionally soft does not necessarily lead to an overall torsionally soft blade, and it may be necessary to modify the skin layup to achieve the desired amount of bend-twist coupling.

1.3.3 Biased Skins and Biased Spar Caps

This design combines the two approaches above, with both the skins and the spar caps contributing to the bend-twist coupling.

2. Candidate Composite Materials

2.1 Stitched Hybrid Fabric

The initial fabric architecture considered in this study consisted of carbon fibers at a +20° angle, and fiberglass fibers at -70° angle. For fabric stability and handling, it was assumed that a small amount of stabilizing fiber would be included in a third direction.

GEC worked with Saertex USA, LLC to develop specifications and cost estimates for a custom stitched fabric with this architecture. The initial cost estimates assumed a total fabric areal weight of 923 grams per square meter (gsm), with 613 gsm of carbon fiber at +22.5°, 300 gsm of E-glass at -70°, 4 gsm of 0° E-glass for stabilization, and 6 gsm of polyester stitching. Taking in account the density of the fibers, this material has 70% carbon content and 30% fiberglass content by volume. Based on an assumed production rate of 325 metric tons per year, Saetrex quoted this fabric at $17.82 / kg, which reflects a relatively high degree of processing efficiency. In practice, the Saertex stitching process is unable to include non-zero angles smaller than ± 22.5°. However, this limitation was confirmed relatively late in this project and a nominal orientation angle of 20° has been assumed for the carbon fibers for all the analyses presented.

Candidate blade designs were developed using this initial stitched fabric architecture. The initial results showed marginal promise for cost-effective manufacture of adaptive blades, particularly for designs in which the biased hybrid fabric is providing the primary structural strength. This can be explained by Table 4, which summarizes the modulus and strength estimates made by J. Mandell for a 0° / 90° carbon / fiberglass hybrid laminate at varying rotation angles.[4] The table indicates that while the compressive strain limits change only modestly with rotation angle, the modulus for supporting flapwise bending loads (E_x) and the corresponding strength drops rapidly.

Table 1. Effect of Rotation Angle on Modulus and Strength (carbon / glass orthotropic laminate)

Rotation Angle (Deg.)	E_x (Gpa)	E_y (Gpa)	G_{xy} (Gpa)	ν_{xy}	Compressive Strain Limits		Relative Flap Bending Strength
					Strain (%)	Failure Mechanism	
0	69.7	13.7	2.87	0.149	0.90	Carbon fiber comp.	1.00
10	42.3	12.7	3.14	0.408	0.85	Shear in glass layer	0.57
20	20.9	10.7	4.12	0.598	0.91	Shear in glass layer	0.30

Following these initial results, GEC investigated alternative candidate architectures for stitched hybrid fabrics. Mechanical properties were calculated using spreadsheet analyses that were checked against the commercial CompositePro code. Some results of this investigation are summarized in Table 2. For all cases the carbon fiber content is 75% by volume at a fixed angle of 20°, and the table indicates the strength and stiffness at varying fiberglass orientation angles. The "relative flap bending strength" in Table 2 uses the same baseline properties as Table 1 (carbon / glass orthotropic laminate at zero rotation). The extent of effective bend-twist coupling is indicated by the shear-coupling coefficient, $\eta_{x,xy}$, which is a measure of the amount of shear strain generated in the xy plane per unit strain in the x-direction. Reviewing the failure mechanisms listed in Table 2, it is seen that transverse stress is the governing criterion for nearly every configuration of biaxial fabric considered. The best combination of strength, stiffness, and coupling occurs

for the fabric with the fiberglass at 0° orientation. However, even for this case the relative flap bending strength is only half of that for the unrotated orthotropic fabric.

Table 2. Combination of 20° Carbon Fibers with Fiberglass at Varying Orientation Angles

Fiberglass Angle (Deg.)	E_x (Gpa)	E_y (Gpa)	G_{xy} (Gpa)	ν_{xy}	$\eta_{x,xy}$	Characteristic Strain Limits		Relative Flap Bending Strength
						Strain (%)	Failure Mechanism	
70	22.2	11.6	3.89	0.15	-1.78	0.26	Transverse to glass fibers	0.09
35	20.8	7.5	3.90	0.41	-1.75	0.40	Transverse to glass fibers	0.13
0	26.3	6.9	4.29	0.56	-1.76	1.17	Transverse to carbon fibers	0.49
-15	30.0	6.9	5.29	0.70	-1.56	0.55	Transverse to glass fibers	0.26
-30	29.3	7.1	5.95	0.85	-1.42	0.50	Transverse to glass fibers	0.23
-45	25.6	7.7	5.60	0.88	-1.47	0.75	Transverse to glass fibers	0.31
-60	22.2	9.2	4.65	0.75	-1.62	0.92	Shear in glass layer	0.33

Calculations were also performed to assess the effect of including a small amount of fiber at a third orientation angle for the purpose of stabilizing the fabric for handling. When fiberglass properties were assumed for the stabilizing fibers, the calculations predicted matrix failure in that layer at a strain level much lower than for the primary carbon and fiberglass layers. This illustrated a general concept concerning the candidate materials under consideration. For the biaxial fabrics listed in Tables 1 and 2, the effective bend-twist coupling is accompanied by relatively large strains in the matrix. However, stiff fibers such as carbon and fiberglass do not accommodate large tensile strains transverse to the fibers. As a consequence the transverse stress limit criterion governed most fabrics considered, even when the ply for which first-ply failure was predicted carried virtually no load.

It is possible that a more elastic fiber, such as polyester, could be used in a stabilizing third-axis orientation without initiating matrix cracking under load. Another possibility is that a biaxial fabric is preimpregnated immediately after stitching, and the B-stage resin could provide stabilization of the fabric during the cutting and handling required for blade manufacture.

Based on the analyses above, two stitched hybrid fabric architectures were selected for evaluation in the parametric analyses of Section 3.0. Both fabrics are 75% carbon and 25% fiberglass by volume, and in both cases the carbon fibers are at a 20° orientation. The fiberglass orientations considered are -70° and 0°, with the mechanical properties as shown in Tables 1 and 2, respectively.

2.2 Oriented Non-Continuous Carbon Fibers

The second material type considered is a carbon preform constructed from non-continuous carbon fibers with a high degree of orientation that is under development by the National Composites Center.[5] Baseline cost estimates and mechanical properties for this "P-4A" perform in a conventional (unbiased) spar cap structure were estimated during the work of Reference 2. For evaluation in the present work, GEC used laminate theory to develop the mechanical properties of P-4A in a rotated orientation. Characteristic strength (strain) values were estimated based on the trends seen for the hybrid fabrics considered above. One potentially favorable attribute of this material is that the orientation angle and perform thickness can be tailored in both the chordwise and spanwise directions with minimal additional processing costs.

3. Parametric Study of Candidate Structural Configurations

A parametric study was performed using the materials identified in the previous section in varying structural arrangements. For each candidate configuration, a constant cross-section blade model was developed and analyzed. Each design was evaluated on the basis of estimated weight, manufacturing cost, and magnitude of bend-twist coupling achieved. On the basis of this parametric study, the most promising combination of materials and structural arrangement was identified and a full-blade model developed.

3.1 Baseline Section Structural Definition

The baseline structural arrangement was selected under the work of References 1 and 2 as being representative of current commercial blade designs. The primary structural member is a box-spar, with webs at 20% and 45% chord and build-up of spar cap material between the webs. The exterior skins and internal shear webs are both sandwich construction with triaxial fiberglass laminate separated by balsa core. This arrangement is depicted in Figure 1, where airfoil section used for the present calculation (25% span station) is shown. For the 1.5 MW rotor, the blade section has a chord of 2.8 m and a maximum thickness of 0.84 m.

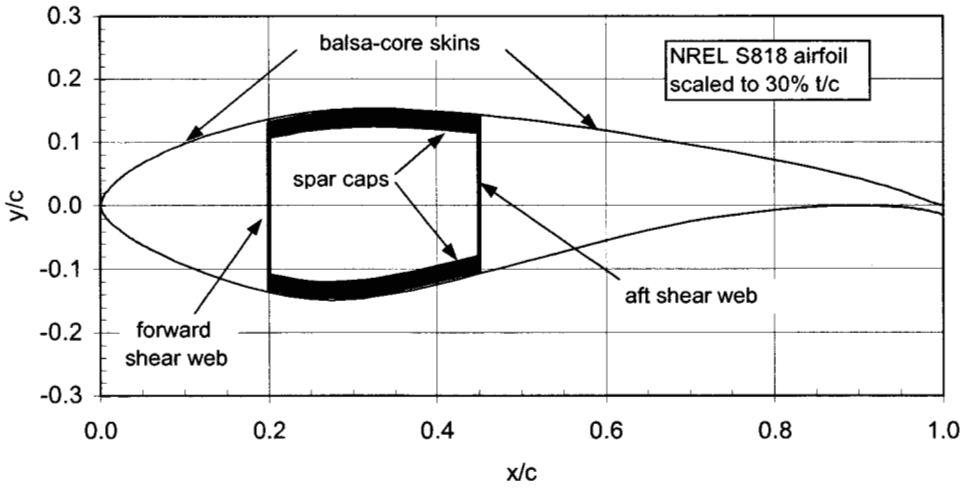

Figure 1. Arrangement of baseline structural model

Table 3 lists the layers in the baseline structural shell and describes the material contained in each. The shear web cores (balsa) are assumed to be 1% of airfoil chord (c) thick, with triaxial skins of 1.27 mm. The skins and spar cap are E-glass/epoxy laminate. The triaxial fabric is designated CDB340, and has a 25%, 25%, and 50% distribution of +45°, -45°, and 0° fibers, respectively. The spar cap is composed of alternating layers of triaxial and uniaxial (A260) fabric. This stacking sequence results in spar cap laminate with 70% uniaxial and 30% off-axis fibers by weight.

Table 3. Baseline Structural-Shell Definition

Layer #	Material	Thickness
1	gel coat	0.51 mm
2	random mat	0.38 mm
3	triaxial fabric	1.27 mm
4		
0%-15% c	balsa	14.0 mm
15%-45% c	spar cap mixture	28.5 mm
45%-85% c	balsa	28.0 mm
5	triaxial fabric	1.27 mm

3.2 Material Properties

Strain-based values for characteristic strength were derived at MSU for the baseline E-glass/epoxy laminate using a combination of test data and laminate theory.[6,7] Following the approach described in Reference 2, material partial safety factors were developed based on the values specified by the Germanischer Lloyd guidelines.[8]

Table 4 summarizes the values for characteristic and design laminate strength that were used to develop the structural designs for both the baseline blade and the configurations with bend-twist coupling. With the exception of the P-4A discontinuous carbon preform, a prepreg material form was assumed. The mechanical properties assume fiber volume fractions of $v_f = 0.45$ for all the carbon / fiberglass hybrid materials, $v_f = 0.5$ for the triaxial fiberglass, and $v_f = 0.55$ for the P-4A discontinuous carbon.

Table 4 Laminate Mechanical Properties and Strength Data

	Elastic constants (GPa)			ν_{xy}	Density	Char. Strength (%)		Design Strength (%)	
Description	Ex	Ey	Gxy	(N.D)	(kg/m^3)	Tension	Comp.	Tension	Comp.
Fiberglass unidirectional + biax, unbiased	29.0	10.2	6.0	0.31	1880	2.70	1.55	1.10	0.63
Carbon uni + glass biax, unbiased	70.8	9.1	4.1	0.35	1562	1.35	0.90	0.55	0.37
Carbon + glass orthotropic, unbiased	69.7	13.7	2.9	0.15	1562	1.35	0.90	0.55	0.37
+20 deg. Carbon, -70 deg. Fiberglass	20.9	10.7	4.1	0.60	1562	0.91	0.91	0.37	0.37
+20 deg. Carbon, 0 deg. Fiberglass	26.3	6.9	4.3	0.56	1562	1.17	1.17	0.48	0.48
P-4A discontinuous carbon, 20 deg. bias	40.5	18.2	7.9	0.62	1540	1.35	1.00	0.51	0.37

Table 5 shows estimates of material and production costs that were developed for the materials considered. These estimates are based on the work of Reference 2 and on subsequent conversations with manufacturers of composite materials and structures.

Table 5 Estimated Cost of Blade Laminate

	Estimated Production Cost ($/kg)	
Description	Material	Finished Blade
Fiberglass triaxial skins	$4.78	$9.58
Fiberglass spar cap laminate	$4.58	$9.28
Unbiased carbon / fiberglass hybrid spar cap	$11.42	$15.92
Biased carbon / fiberglass laminate (spar cap or skins)	$13.12	$17.62
NCC P-4A discontinuous oriented carbon	$19.20	$20.45

3.3 Calculation of Blade Section Structural Properties

Using the NuMAD interface, an ANSYS finite-element model was constructed for each configuration evaluated. Each model had the general sectional layout as indicated in Figure 1. In all cases the shear webs were balsa core with triaxial fiberglass facings. Each blade design also had balsa-core skins with an outer layer of gel coat and veil mat. The facings of the outer blade section skins and the spar cap laminate were modified per each configuration modeled.

Each blade design evaluated was modeled within ANSYS as a cantilevered beam of 20 meter length with constant cross-section dimensions. A tip load was applied, and the strains at the midspan evaluated for a 50-year Class 1 extreme gust per the IEC 61400-1 standard.[9] Based on the results, the thickness of the spar cap laminate was adjusted iteratively until the design strain levels of Table 4 were satisfied. The convergence criteria used was that the critical laminate strain under load must be within 0.5% of the design value. In all cases, the compressive strain governed the structural designs.

Once the blade structure had been sized, the structural properties for each configuration were calculated by evaluating the displacements at the mid-span of a cantilevered beam under unit bending loads. Equation set (9) of Reference 10 was used, introducing the notation:

M_B ≡ Flapwise bending moment (N-m)
M_T ≡ Torsional bending moment (N-m)
δ ≡ Displacement in flapwise direction (m)
ϕ_T ≡ Torsional displacement due to M_T (rads)
ϕ_B ≡ Torsional displacement due to M_B (rads)
EI ≡ Flapwise bending stiffness (N-m^2)
GJ ≡ Torsional bending stiffness (N-m^2)
α ≡ Bend-twist coupling coefficient (non-dimensional)
L ≡ Length of beam from fixed end to section under evaluation (m)

Equation set (9) of Reference 10 can then be arranged as:

$$\alpha = \phi_B \sqrt{\frac{M_T}{M_B}\frac{L}{2\cdot\delta\cdot\phi_T}} \qquad \text{(Eqn. 1)}$$

$$EI = \frac{1}{1-\alpha^2}\frac{L^2\cdot M_B}{2\cdot\delta} \qquad \text{(Eqn. 2)}$$

$$GJ = \frac{1}{1-\alpha^2}\frac{L\cdot M_T}{\phi_T} \qquad \text{(Eqn. 3)}$$

The overall equivalent bend-twist coupling κ_{equiv} (in units of degrees twist per meter span, per N-m of flapwise bending moment) can be derived by rearranging Equation 3 in the form:

$$\kappa_{equiv} = 57.3\cdot\frac{\phi_T}{M_T\cdot L} = \frac{57.3}{(1-\alpha^2)\cdot GJ} \qquad \text{(Eqn. 4)}$$

3.4 Parametric Study Results and Discussion

Table 6 provides a summary of the structural properties and cost estimates for the configurations modeled. Unless specifically noted otherwise, "biased hybrid" materials have carbon fibers at an orientation of 20° and glass fiber at an orientation of -70°. Although the weight and cost are evaluated on a unit span basis, it is expected that similar trends would results at other blade spanwise stations that incorporate bend-twist coupling. In the following discussion all numerical comparisons will be made relative to the all-fiberglass baseline (case #1)

The baseline carbon / fiberglass hybrid design with no coupling (case #2) has spar caps that are 35% thinner than the all-fiberglass baseline. Consequently the cost increase for the carbon / fiberglass hybrid design is only about 1%. Also, the design strain (static compressive) is 0.63%for the all-fiberglass baseline and only 0.37% for the unbiased hybrid spar cap. As a result, the hybrid baseline blade would have 35% lower tip deflections under a given bending load than the all-fiberglass baseline. The conclusion is that for a conventional blade, the carbon / fiberglass spar cap is competitive with, and perhaps superior to, the all-fiberglass baseline in terms of cost and structural properties.

The relative merit of the seven bend-twist configurations considered is less clear. The configurations have varying degrees of bend-twist coupling, but show cost increases ranging from 34% to 250% above the baseline. For all the cases with biased spar caps, significant cost increases result from the need for relatively thick spar cap laminate. A comparison of cases #3 and #4 shows the benefit of improved load carrying capability of biased spar materials. For a spar cap constructed of 20° carbon with -70° fiberglass (case #3), the cost increase over the baseline is 195%. By shifting the fiberglass to 0° (case #4), the cost increase drops to 76%, and the effective coupling is increased 35%. The configuration with fiberglass skins and a biased spar cap manufactured from P-4A non-continuous carbon (case #8) shows a cost increase of 68% over the baseline, but a lower effective coupling value than configuration #4.

The case with biased skins and a fiberglass spar (case #5) is not promising, with a 90% cost increase and the lowest effective coupling. This can be attributed to the mismatch in design strains between the biased skin and fiberglass spar materials. With a design strain of 0.37%, the biased skin material governs the section design. The fiberglass material has a design strain of 0.63%, but is limited to 0.37% so that the skin design strains are not exceeded. As a result, a substantial amount of fiberglass material is required and the spar caps are more than twice the thickness of case #1.

Of the configurations considered, the best combination of cost and bend-twist coupling is biased hybrid skins with an unbiased hybrid spar cap (case #6). The effective coupling is less than case #4, but the cost increase is only 34% over the baseline. The modest cost increase is primarily a function of good matching between the skin and spar cap design strains. The unbiased hybrid spar of case #6 is nominally the same as for the non bend-twist hybrid baseline (case #2).

Using the skins rather than the spar cap structure to initiate the bend-twist coupling has additional benefits concerning load paths and stress concentrations. It is expected that the biased fibers in the skins could be curtailed prior to the leading and trailing edges to avoid stress / strain discontinuities there. Because the unbiased spars would be carrying the majority of the bending loads, the stress concentrations at the biased skin drop-offs should be modest. Also, the leading and trailing edges are near the flapwise elastic axis so curtailing the biased fibers in this region should have minimal effect on the coupling achieved. By contrast if a spar cap is providing both bend-twist coupling and flapwise bending strength, it would be much more challenging to avoid large stress concentrations and matrix-dominated load paths.

Table 6. Structural Properties and Estimated Costs for Bend-Twist Blade Configurations

		Spar Cap Thickness		Mass	EI	GJ	α	κ_{equiv}	Prod. Cost ($/m)	
	Configuration	(mm)	(% T)	(kg/m)	($N-m^2$)	($N-m^2$)		(deg./$N-m^2$)	Material	Total
#1	Baseline fiberglass skins and spar cap	28.5	3.4	148	2.35E8	4.48E7	-	-	$695	$1,400
#2	Baseline with carbon / glass hybrid spar	24.6	2.9	118	4.05E8	4.03E7	-	-	$885	$1,415
#3	Fiberglass skins with +20° / -70° hybrid spar	95.0	11.3	267	4.17E8	4.93E7	.195	8.1E-8	$2,925	$4,125
#4	Fiberglass skins with +20° / 0° hybrid spar	50.0	5.3	173	3.28E8	4.72E7	.228	1.1E-7	$1,690	$2,465
#5	Biased hybrid skins with fiberglass spar	63.0	7.5	224	4.04E8	5.25E7	.136	5.4E-8	$1,580	$2,665
#6	Biased hybrid skins with unbiased hybrid spar	23.5	2.8	111	4.08E8	4.60E7	.162	7.0E-8	$1,375	$1,870
#7	Biased hybrid skins and +20° / -70° hybrid spar	101.5	12.1	276	4.41E8	5.66E7	.311	1.2E-7	$3,615	$4,855
#8	Fiberglass skins with P-4A biased spar cap	43.2	5.1	157	4.08E8	4.79E7	.165	7.0E-8	$2,010	$2,345
#9	Biased hybrid skins with P-4A biased spar	45.0	5.4	156	4.28E8	5.47E7	.286	1.2E-7	$2,600	$3,010

4. Complete Adaptive Blade Model

Based on the parametric analysis results, a configuration comprised of biased hybrid skins with an unbiased hybrid spar cap (case #6) was selected for constructing a structural model for a complete adaptive blade. This design was developed in conjunction with the WindPACT Rotor System Design Study. The planform and twist distribution for the blade are listed in Table 7. The peak bending loads used in the initial design were based on aeroelastic simulation results from the rotor study (for a carbon fiberglass hybrid blade with no bend-twist coupling). Figure 2 shows an ANSYS model of the complete blade. For reference, the turbine system power and rotor speed curves are given in Figure 3.

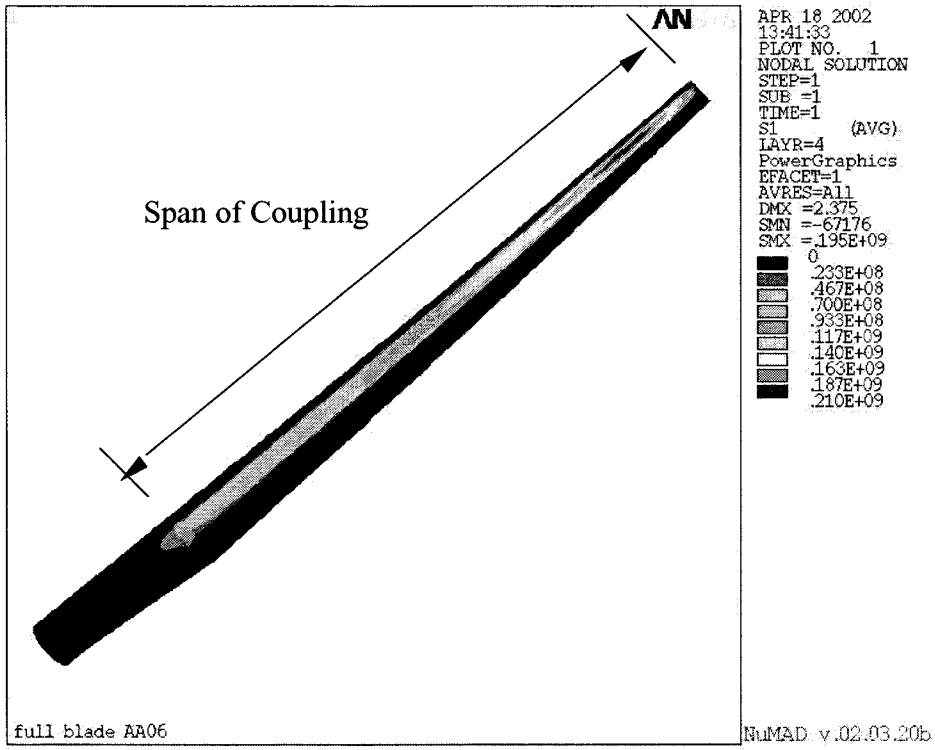

Figure 2. ANSYS Model of Complete Adaptive Blade

Table 7. Planform and Mass / Cost Summary for Initial Adaptive Blade Design

					Baseline Hybrid Blade		Adaptive Blade	
Spanwise Station		Chord		Twist	Unit Mass	Unit Cost	Unit Mass	Unit Cost
r/R	(m)	c/R	(m)	(Deg.)	(kg/m)	($/m)	(kg/m)	($/m)
0.05	1.75	0.055	1.925	10.4	1074	9,965	1074	9,965
0.07	2.45	0.055	1.925	10.4	182	1,690	182	1,690
0.25	8.75	0.070	2.450	10.4	81.8	1,000	78.5	1,300
0.50	17.50	0.056	1.970	2.5	61.6	765	57.3	950
0.75	26.25	0.043	1.500	0.0	35.5	400	32.5	530
1.00	35.00	0.030	1.064	-0.6	12.5	115	11.2	185
				Totals =	**2530 kg**	**$27,625**	**2440 kg**	**$32,945**
				Plus Root Connection =		**$32,625**		**$37,945**

Table 7 lists the mass and cost calculated at each spanwise station for both the baseline (non-adaptive carbon / fiberglass hybrid) and the adaptive blade. It was assumed that the biased spar material starts at the 25% span location and that both blades are of identical fiberglass construction between 25% span and the root. Between 25% and 75% span the unit cost of the adaptive blade is 24% to 33% higher than the baseline blade. However, a significant portion of the total blade weight and cost is located between the root and 25% span. As a result, the cost for the complete adaptive blade structure is estimated as only 19% higher than the baseline blade. When $5,000 is added to each design for the root-connection, the differential for the complete blade assembly is only 16%.

Table 8 gives the structural properties for the adaptive blade sections and also tabulates the mean flapwise bending load and resulting blade twist at a schedule of wind speeds. Significant bend-twist coupling is achieved with this design. At 12 m/s wind speed, the mean change in twist angle is 3.1° and 4.1°, respectively, at the 75% span station and the blade tip. Above rated, the blade is pitched to feather for power control and the mean flapwise bending loads decrease substantially. However, the blade will still respond in an adaptive way, such that an increase in bending loads will result in additional blade twist to feather.

The blade design presented here, and derivatives of this design, are currently being evaluated via aeroelastic simulations as part of the WindPACT rotor study. Although these evaluations are not complete, the results appear promising for reductions in system loads and cost of energy.

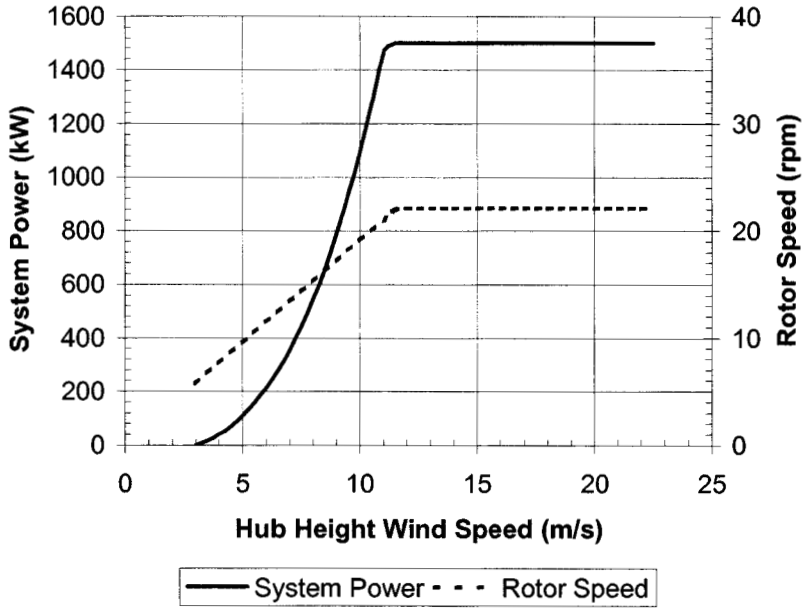

Figure 3. Power and Rotor Speed Curves for Adaptive Blade Model

Table 8. Structural Properties for Complete Adaptive Blade

r/R	r (m)	EI_{Flap}	GJ	α	κ_{XY}	V = 8 m/s		V = 12 m/s		V = 16 m/s		V = 20 m/s		V = 24 m/s	
						M_{Flap} (kN-m)	Δ Twist (deg./m)	M_{Flap} (kN-m)	Δ Twist (deg./m)	M_{Flap} (kN-m)	Δ Twist (deg./m)	M_{Flap} (kN-m)	Δ Twist (deg./m)	M_{Flap} (kN-m)	Δ Twist (deg./m)
0.25	8.75	2.05E+08	3.04E+07	0.189	1.42E-07	889	0.126	1272	0.181	842	0.120	600	0.085	448	0.064
0.50	17.50	6.28E+07	9.95E+06	0.191	4.54E-07	249	0.113	335	0.152	182	0.083	81	0.037	5	0.002
0.75	26.25	1.24E+07	3.00E+06	0.272	2.76E-06	62	0.171	83	0.229	38	0.105	8	0.022	-15	-0.041
Total Δ Twist at 75% Span (deg.) =							**2.3**		**3.1**		**1.7**		**0.8**		**0.1**
Total Δ Twist at Tip (deg.) =							**3.0**		**4.1**		**2.2**		**0.9**		**-0.1**

5. Conclusions

A number of candidate fiber orientations and fabric architectures for adaptive blade manufacture have been identified and assessed on the basis of estimated static strength, stiffness, and fabrication costs. The results illustrate the difficulty of achieving good bend-twist characteristics while maintaining stiffness and strength.

A parametric study was performed to evaluate candidate fabric types and structural arrangements. The results indicate:

- Configurations that incorporate adaptive materials in the spar cap provide the most effective coupling. However, the cost premium resulting from the relatively low strength of the adaptive materials is likely to be prohibitive.
- Large cost increases were seen for all designs in which there is a significant mismatch between the design strain values for the skins and spar cap laminate.
- The best combination of effective coupling and cost was achieved for the configuration comprised of biased hybrid skins with an unbiased hybrid spar cap.

A complete adaptive blade model was developed for this configuration. The blade assembly was estimated to cost only 16% more than the baseline design. Based on a static bending-load evaluation, a significant amount of bend-twist coupling is achieved with this design. Results from the initial aeroelastic simulations performed under the WindPACT Rotor System Design Study indicate that the bend-twist coupling results in a meaningful reduction in rotor system loads.

6. References

1. Malcolm, D., Hansen C. (June 2001) *Results from the WindPACT Rotor Design Study*. Proceedings Windpower 2001, American Wind Energy Association, Washington DC.
2. Griffin, D.A. (publication pending). *Blade System Design Studies Volume I: Composite Technologies for Large Wind Turbine Blades*. Albuquerque, NM: Sandia National Laboratories.
3. Laird, D.L. (January 11-14 2001). *2001: A Numerical Manufacturing and Design Tool Odyssey*. Proceedings of AIAA/ASME Wind Energy Symposium. Reno, NV.
4. Mandell, J.F. (November 3, 2001), Estimated static strength and mechanical properties for hybrid carbon / fiberglass laminate at varying rotation angles, email communication with GEC.
5. Reeve, S., Cordell, T. (May 6-10 2001). *Carbon Fiber Evaluation for Directed Fiber Preforms*. Proceedings of the 46th International SAMPE Symposium and Exhibition.
6. Mandell, J.F., Samborsky, D.D. (1997). "*DOE/MSU Composite Material Fatigue Database: Test Methods, Materials and Analysis*." SAND97-3002.
7. Mandell, J.F. (March 10, 2001), Estimated static strength and mechanical properties for GEC trade-off study on spar cap materials, email communication with GEC.
8. Germanischer Lloyd. (1999). Rules and Regulations IV—Non-Marine Technology, Part 1—Wind Energy, *Regulation for the Certification of Wind Energy Conversion Systems*.
9. International Electrotechnical Commission. (1999). *IEC 61400-1: Wind turbine generator systems—Part 1: Safety Requirements*, 2nd Edition. International Standard 1400-1.
10. Lobitz D.W., Veers, P.S. (January 1998), *Aeroelastic Behavior of Twist-Coupled HAWT Blades*, Proceedings of AIAA/ASME Wind Energy Symposium. Reno, NV.

DISTRIBUTION

H. Ashley
Dept. of Aeronautics and
Astronautics Mechanical Engr.
Stanford University
Stanford, CA 94305

K. Bergey
University of Oklahoma
Aero Engineering Department
Norman, OK 73069

D. Berry
TPI Composites Inc.
373 Market Street
Warren, RI 02885

R. Blakemore
GE Wind
13681 Chantico Road
Tehachapi, CA 93561

C. P. Butterfield
NREL
1617 Cole Boulevard
Golden, CO 80401

G. Bywaters
Northern Power Systems
Box 999
Waitsfield,VT 05673

J. Cadogan
Office of Wind and Hydro Technology
EE-12
U.S. Department of Energy
1000 Independence Avenue SW
Washington, DC 20585

D. Cairns
Montana State University
Mechanical & Industrial Engineering Dept.
220 Roberts Hall
Bozeman, MT 59717

S. Calvert
Office of Wind and Hydro Technology
EE-12
U.S. Department of Energy
1000 Independence Avenue SW
Washington, DC 20585

J. Chapman
OEM Development Corp.
840 Summer St.
Boston, MA 02127-1533

Kip Cheney
PS Enterprises
222 N. El Segundo, #576
Palm Springs, CA 92262

C. Christensen, Vice President
GE Wind
13681 Chantico Road
Tehachapi, CA 93561

R. N. Clark
USDA
Agricultural Research Service
P.O. Drawer 10
Bushland, TX 79012

C. Cohee
Foam Matrix, Inc.
1123 East Redondo Blvd.
Inglewood, CA 90302

J. Cohen
Princeton Economic Research, Inc.
1700 Rockville Pike
Suite 550
Rockville, MD 20852

C. Coleman
Northern Power Systems
Box 999
Waitsfield, VT 05673

K. J. Deering
The Wind Turbine Company
515 116th Avenue NE
No. 263
Bellevue, WA 98004

A. J. Eggers, Jr.
RANN, Inc.
744 San Antonio Road, Ste. 26
Palo Alto, CA 94303

D. M. Eggleston
DME Engineering
1605 W. Tennessee Ave.
Midland, TX 79701-6083

P. R. Goldman
Director
Office of Wind and Hydro Technology
EE-12
U.S. Department of Energy
1000 Independence Avenue SW
Washington, DC 20585

D. Griffin (5)
GEC
5729 Lakeview Drive NE, Ste. 100
Kirkland, WA 98033

C. Hansen
Windward Engineering
4661 Holly Lane
Salt Lake City, UT 84117

C. Hedley
Headwaters Composites, Inc.
PO Box 1073
Three Forks, MT 59752

S. Hock
Wind Energy Program
NREL
1617 Cole Boulevard
Golden, CO 80401

D. Hodges
Georgia Institute of Technology
270 Ferst Drive
Atlanta, GA 30332

Bill Holley
3731 Oakbrook
Pleasanton, CA 94588

K. Jackson
Dynamic Design
123 C Street
Davis, CA 95616

E. Jacobsen
GE Wind
13000 Jameson Rd.
Tehachapi, CA 93561

G. James
University of Houston
Dept. of Mechanical Engineering
4800 Calhoun
Houston, TX 77204-4792

M. Kramer
Foam Matrix, Inc.
PO Box 6394
Malibu CA 90264

A. Laxson
NREL
1617 Cole Boulevard
Golden, CO 80401

S. Lockard
TPI Composites Inc.
373 Market Street
Warren, RI 02885

J. Locke, Associate Professor
Wichita State University
207 Wallace Hall, Box 44
Wichita, KS 67620-0044

D. Malcolm
GEC
5729 Lakeview Drive NE, Ste. 100
Kirkland, WA 98033

J. F. Mandell
Montana State University
302 Cableigh Hall
Bozeman, MT 59717

T. McCoy
GEC
5729 Lakeview Drive NE, Ste. 100
Kirkland, WA 98033

L. McKittrick
Montana State University
Mechanical & Industrial Engineering Dept.
220 Roberts Hall
Bozeman, MT 59717

P. Migliore
NREL
1617 Cole Boulevard
Golden, CO 80401

A. Mikhail
Clipper Windpower Technology, Inc.
7985 Armas Canyon Road
Goleta, CA 93117

W. Musial
NREL
1617 Cole Boulevard
Golden, CO 80401

NWTC Library (5)
NREL
1617 Cole Boulevard
Golden, CO 80401

B. Neal
USDA
Agricultural Research Service
P.O. Drawer 10
Bushland, TX 79012

V. Nelson
Department of Physics
West Texas State University
P.O. Box 248
Canyon, TX 79016

T. Olsen
Tim Olsen Consulting
1428 S. Humboldt St.
Denver, CO 80210

R. Z. Poore, President
Global Energy Concepts, Inc.
5729 Lakeview Drive NE
Suite 100
Kirkland, WA 98033

R. G. Rajagopalan
Aerospace Engineering Department
Iowa State University
404 Town Engineering Bldg.
Ames, IA 50011

J. Richmond
MDEC
3368 Mountain Trail Ave.
Newbury Park, CA 91320

Michael Robinson
NREL
1617 Cole Boulevard
Golden, CO 80401

D. Sanchez
U.S. Dept. of Energy
Albuquerque Operations Office
P.O. Box 5400
Albuquerque, NM 87185

R. Sherwin
Atlantic Orient
PO Box 1097
Norwich, VT 05055

Brian Smith
NREL
1617 Cole Boulevard
Golden, CO 80401

J. Sommer
Molded Fiber Glass Companies/West
9400 Holly Road
Adelanto, CA 93201

K. Starcher
AEI
West Texas State University
P.O. Box 248
Canyon, TX 79016

F. S. Stoddard
79 S. Pleasant St. #2A
Amherst, MA 01002

A. Swift
University of Texas at El Paso
320 Kent Ave.
El Paso, TX 79922

J. Thompson
ATK Composite Structures
PO Box 160433
MS YC14
Clearfield, UT 84016-0433

R. W. Thresher
NREL
1617 Cole Boulevard
Golden, CO 80401

S. Tsai
Stanford University
Aeronautics & Astronautics
Durand Bldg. Room 381
Stanford, CA 94305-4035

W. A. Vachon
W. A. Vachon & Associates
P.O. Box 149
Manchester, MA 01944

C. P. van Dam
Dept of Mech and Aero Eng.
University of California, Davis
One Shields Avenue
Davis, CA 95616-5294

B. Vick
USDA, Agricultural Research Service
P.O. Drawer 10
Bushland, TX 79012

K. Wetzel
K. Wetzel & Co., Inc.
PO Box 4153
4108 Spring Hill Drive
Lawrence, KS 66046-1153

R. E. Wilson
Mechanical Engineering Dept.
Oregon State University
Corvallis, OR 97331

M. Zuteck
MDZ Consulting
601 Clear Lake Road
Clear Lake Shores, TX 77565

M.S. 0557	T. J. Baca, 9125
M.S. 0557	T. G. Carne, 9124
M.S. 0708	H. M. Dodd, 6214 (25)
M.S. 0708	T. D. Ashwill, 6214 (10)
M.S. 0708	D. E. Berg, 6214
M.S. 0708	R. R. Hill, 6214
M.S. 0708	P. L. Jones 6214
M.S. 0708	D. L. Laird, 6214
M.S. 0708	D. W. Lobitz, 6214
M.S. 0708	M. A. Rumsey, 6214
M.S. 0708	H. J. Sutherland, 6214
M.S. 0708	P. S. Veers, 6214
M.S. 0708	J. Zayas, 6214
M.S. 0847	K. E. Metzinger, 9126
M.S. 0958	M. Donnelly, 14172
M.S. 1490	A. M. Lucero, 12660
M.S. 0612	Review & Approval Desk, 9612 For DOE/OSTI
M.S. 0899	Technical Library, 9616 (2)
M.S. 9018	Central Technical Files, 8945-1